# Molecular structure and ammonia gas adsorption capacity of a Cu (II)-1,10-phenanthroline complex intercalated in montmorillonite by DFT simulations

C. Ignacio Sainz-Díaz [a],[*], Elena Castellini [b], Elizabeth Escamilla-Roa [a], Fabrizio Bernini [b], Daniele Malferrari [b], Maria Franca Brigatti [b], Marco Borsari [b]

[a] *Andalusian Institute of Earth Sciences (CSIC-UGR), Av. de Las Palmeras, 4, 18100-Armilla, Granada, Spain*
[b] *Department of Chemical and Geological Sciences, University of Modena and Reggio Emilia, Via Campi 103, Modena I, 41125, Italy*

A B S T R A C T

A hydrated complex of 1,10-phenanthroline with $Cu^{2+}$ cation was intercalated in the interlayer space of montmorillonite. This intercalation occurs initially by through a cation exchange mechanism in which the charge of the complex cation compensates the excess of the negative charge of the interlayer, then, once the cation exchange capacity (CEC) value has been reached, by direct adsorption of the sulfate salt of this complex (*i.e.* the cation together with its sulfate counterion). This material has showed interesting entrapping properties of gaseous phases and a peculiar chemical reactivity. However, the complete characterization and explanation of the formation of these materials is difficult with only experimental techniques. Hence, we used computational methods at atomic level to know how are the molecular structure of these complexes and their adsorption capacity of ammonia inside the interlayer confined space of montmorillonite for a better understanding of the experimental behaviour. First Principles calculations were performed based on Density Functional Theory (DFT). The intercalation of the phenanthroline-Cu(II) complex inside the nanoconfined interlayer of montmorillonite is energetically favourable in the relative proportion observed experimentally, being a cation exchange process. The further adsorption of the sulfate salt of the phenanthroline-Cu complex is also energetically possible. The adsorption of ammonia molecules in these montmorillonite-phenanthroline-Cu complexes was also favourable according with experimental behaviour.

## 1. Introduction

Clay minerals are one of the most abundant mineral groups in the Earth Biosphere and also are present in other planets. They are present in soils, in the atmosphere and oceans. These natural materials have high absorption capacity with a certain catalytic activity, a small particle size and a great specific surface. Besides they provide confined nanospaces where the chemistry can be different to that in macroscopic spaces. These minerals can act as inorganic membranes with selective adsorption and diffusion properties altering the fluid dynamics through the solid matter. This property and the confined nanospaces offer an excellent scenario for overcoming entropic barriers for the initial pre-biotic reactions and the first step for the origin of the Life [1,2]. Within the clay minerals group, the phyllosilicates have a layered structure with high cation exchange capacity and swelling properties

deriving from the weak interactions in the interlayer space. They can host different molecules in the interlayer space conferring peculiar properties. Organic and inorganic compounds have been immobilized in the interlayer space of 2:1-phyllosilicates with specific properties [3].

Organic-inorganic hybrid compounds are becoming very interesting structures due to their potential applications for photo-, electro- and magnetic-materials and in catalysis, and medicine. The combination of transition metal cations with rigid organic ligands as building blocks is especially attractive [4]. Moreover, the immobilization of these hybrid complexes is very interesting for applications in heterogeneous catalysis and green chemistry where the catalyst can be recovered and re-used in industrial processes. Metal complexes containing 1,10-phenanthroline ligands received wide attention due to their long-standing applications in analytical chemistry [5]. Recently a μ-oxo dinuclear Fe (III)-phenanthroline complex has been studied [6]. Besides, this Fe

complex was intercalated in montmorillonite interlayer increasing the interlayer spacing and the stacking order [7,8], with new properties for adsorption and reactivity at the solid/gas interfaces [9–11].

Very recently Cu(II)-1,10-phenanthroline complexes intercalated in montmorillonite have been studied [12], finding interesting adsorption properties of ammonia [13]. However, some aspects of molecular structure and intermolecular interactions could not be understood completely. In this work, molecular modelling calculations are applied to know the molecular structure of these hybrid materials, especially of the organo-Cu complex into the confined interlayer space of montmorillonite and their adsorption property towards ammonia.

## 2. Methodology and models

First-principles calculations based on the Density Functional Theory (DFT) method were carried out by means of the CASTEP [14] and Dmol3 [15] codes applying periodical boundary conditions in 3-D dimension. Dmol3 is based on localized atomic orbitals, and double-$\zeta$ extended basis sets with polarization functions were used. CASTEP is based on plane waves. The generalized gradient approximation (GGA) and Perdew−Burke−Ernzerhof (PBE) parametrization of the exchange correlation function were applied in both methods and the Tkatchenko-Scheffler [16] dispersion correction was used. Pseudopotentials with semicore correction (DSPP) were used in Dmol3. Ultrasoft pseudopotentials were used in CASTEP. In both methods the polarization of spin was included due to the presence of the Cu cation. The calculations are performed considering the $\Gamma$ point of the Brillouin zone and the convergence threshold criterion for the self-consistent field was $1 \times 10^{-6}$. The optimization of atomic positions and crystal lattice cell parameters was performed at 0 K. In all structures, all atoms and the cell parameters were relaxed by means of conjugated gradient minimizations [17]. These conditions are consistent with previous studies with organics [18], phyllosilicates and other minerals [19,20].

The crystal structure of montmorillonite was taken from previous optimizations [21] with the unit-cell formula: $Ca_{0.33}(Al_{3.5}Mg_{0.5})$ $(Si_{7.75}Al_{0.17})O_{20}(OH)_4$. The chemical composition of this model is close to the montmorillonite STx-1b experimentally used [22] $(Ca_{0.34}Na_{0.04}K_{0.06})$ $(Al_{3.28}Fe^{3+}_{0.14}Mg_{0.56}Ti_{0.02})$ $(Si_{7.75}Al_{0.25})O_{20}(OH)_4$. The initial model of the Cu(II)-1,10-phenanthroline (phenCu) complex was taken from experimental crystallographic data [4]. We extracted one phenCu cation from the crystal lattice structure along with the counter-ion sulfate. This ion-pair was placed in the centre of an empty box with periodical boundary conditions of $20 \times 20 \times 15$ Å for avoiding inter-cell interactions. Considering the dimensions of this Cu-complex, a supercell $3 \times 2 \times 1$ of montmorillonite was used in order to avoid intermolecular interactions with vicinal cells in the periodical model. Hence, the chemical composition of this supercell was $Ca_2(Al_{21}Mg_3)$ $(Si_{47}Al_1)O_{120}(OH)_{24}$. The cation substitutions for the generation of this supercell model were placed considering the high dispersion tendency of Mg cations in this kind of structures according to previous studies [23,24].

## 3. Results and discussion

In the crystal structure of the Cu-1,10-phenanthroline complex, the $Cu^{2+}$ cation is coordinated symmetrically with the phenanthroline N atoms and two water molecules, where $Cu^{2+}$, N atoms and the water O atoms remain in the same plane. The sulfate anions are bridging between two complexes and the $Cu^{2+}$ cation is coordinated with two sulfates sharing them with the vicinal complexes. We extracted this complex from the crystal and placed it in a empty cubic box of $20 \times 20 \times 15$ Å. This complex has the phenanthroline N atoms, $Cu^{2+}$ cation and the water O atoms in the same plane as in the crystal and the sulfate O atoms coordinated with the water H atoms. This complex model was optimized initially with Dmol3 and later was reoptimized with CASTEP. This optimized structure maintained the pristine form with d(SO⋯HO) =

1.374 Å (**phenCu_sulf2w**) (Fig. 1a). However, the $Cu^{2+}$ cations can have also an octahedral six-coordination. Hence, we generated another complex with the water molecules forming a perpendicular axis with respect to the phenanthroline-Cu plane with the water O atoms oriented towards the $Cu^{2+}$ cation and the sulfate O atoms completing the coordination in the same phenanthroline-Cu plane (**phenCu2w_sulf**) (Fig. 1b). This last complex optimized has a d(Cu⋯OH2) = 2.037–2.040 Å, d(Cu⋯N) = 2.042 Å, and d(Cu…OS) = 2.337–2.383 Å. This complex is 7.79 kcal/mol more stable than the above one after the optimization of both isolated complexes. Hence, this last model of the complex (**phenCu2w_sulf**) was selected and used for the rest of this work.

This sulfate complex in aqueous media will be solvated and the minimal solvation sphere will be the phenanthroline-$Cu^{2+}$ cation completing the octahedral coordination with 4 water molecules (**phenCu4w**) (Fig. 1c).

The size of the **phenCu2w_sulf** complex is $10 \times 9 \times 5$ Å$^3$, and that of the **phenCu4w** cation is $9 \times 8.5 \times 6$ Å$^3$. Hence, the $3 \times 2 \times 1$ ($16 \times 18 \times 15$ Å$^3$) supercell of montmorillonite is suitable for the intercalation of these complexes. This supercell has two $Ca^{2+}$ interlayer cations that were hydrated with 6 water molecules each one forming an octahedral coordination for both cations. Hence, this supercell has 12 water molecules. This model was fully optimized regarding atomic positions and cell parameters with variable volume (**mnt2Ca12w**) with CASTEP yielding a d(001) spacing of 14.0 Å being lower than in experiments (15.1 Å) due to the lower amount of water in this model. After the optimization, the distribution of water molecules was disordered, they did not form a perfect octahedral coordination with $Ca^{2+}$ cations in the interlayer space (Fig. 2a). Some water O atoms form the coordination sphere of $Ca^{2+}$ at a distance around 2.3–3.1 Å and the water H atoms form H bonding with the mineral surface O atoms with d(OH⋯OSi) = 2.3–2.7 Å and with other water O atoms with d(OH⋯HO) = 1.66 Å. This model was compared with a periodical box of 12 water molecules and the dry structure of montmorillonite (**mnt2Ca**). The hydration of this montmorillonite in the confined interlayer space was energetically favourable with an energy of −102.7 kcal/mol, −8.56 kcal/mol per water molecule.

In this optimized structure, one intercalated $Ca^{2+}$ hydrated was substituted by one hydrated phenanthroline-$Cu^{2+}$ cation, where the phenanthroline ring is parallel to the interlayer mineral surface (**mntCa6wphenCu4w**). The full optimization of this structure yielded a d(001) spacing of 14.0 Å. The phenanthroline ring remained parallel to the mineral surface but in an inclined plane (Fig. 2b). From this last model the other hydrated $Ca^{2+}$ cation was substituted by one additional phenanthroline-$Cu^{2+}$ cation, where the phenanthroline ring was placed also parallel to the mineral 001 surface (**mnt2phenCu8w**). The optimization of this structure yielded a d(001) spacing of 14.7 Å, maintaining both phenanthroline rings in a parallel orientation with respect to the mineral surface with the hydrophilic groups ($Cu^{2+}$ and water molecules) close each other and the hydrophobic (phenanthroline) moieties together in opposite side (Fig. 2c). In both complexes, each $Cu^{2+}$ cation is penta-coordinated with the 2 phenanthroline N atoms, d(N⋯Cu) = 1.95–2.01 Å, and 3 water molecules, d(HO⋯Cu) = 2.0–2.19 Å. The other water molecules went towards the mineral surface forming strong H bonds d(HOH⋯OSi) = 1.60–1.91 Å. Additional H bonds exist between the water molecules d(HO⋯HO) = 1.60–2.1 Å. This structure can describe the atomic arrangement of the hybrid composite obtained experimentally and described as semisaturated complex in previous work [13].

The formation of both former complexes (**mntCa6wphenCu4w** and **mnt2phenCu8w**) is produced by means of a cation exchange mechanism. To evaluate the energetic of this reaction we have to include a model that represents the $Ca^{2+}$ cation outside the mineral interlayer. For that we generated a periodical box model of the $Ca^{2+}$ cation with the sulfate anion, and this ion-pair was solvated with 6 water molecules for the $Ca^{2+}$ cation, like in the mineral interlayer, and 4 water molecules for the sulfate (**Casulf10w**). In the same way, we prepared a model of a
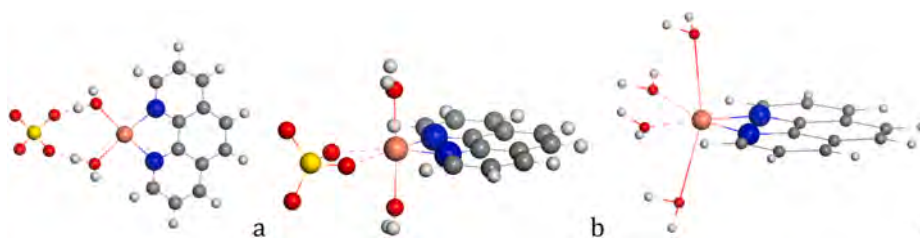
**Fig. 1.** Cu-1,10-phenanthroline complexes, sulfate in planar conformation (a), sulfate in octahedral coordination (b), and the free cation form coordinated with 4 water molecules (c). The H, C, N, Cu, O, and S atoms are in clear-gray, gray, blue, pink, red, and yellow colours, respectively. This colour criterium is extended to the rest of this work. (For interpretation of the references to colour in this figure legend, the reader is referred to the Web version of this article.)
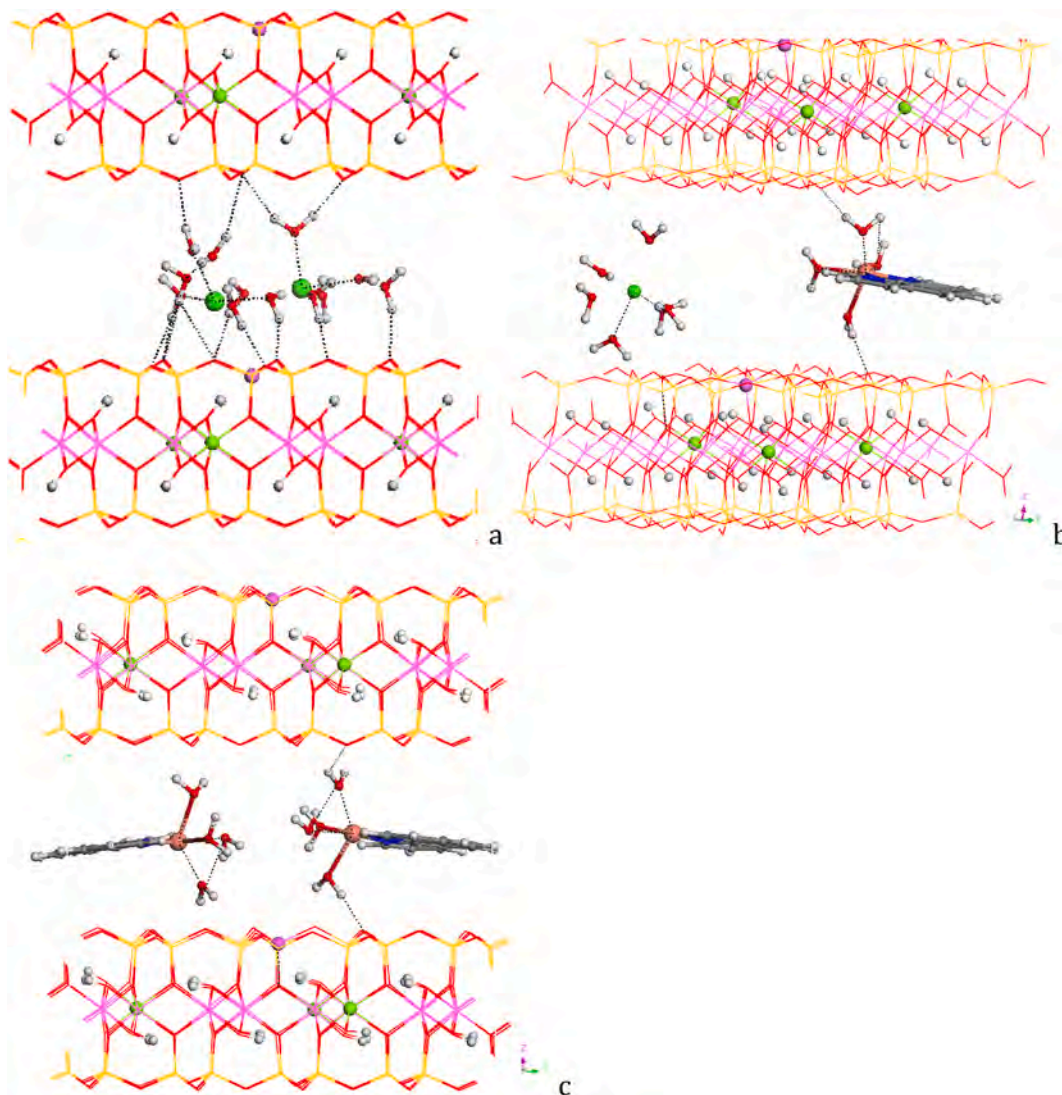


**Fig. 2.** Optimized structures of the montmorillonite intercalated with only $Ca^{2+}$ (a, **mnt2Ca12w**), with one phenCu$^{2+}$ (b, **mntCa6wphenCu4w**) and two phenCu$^{2+}$ (c, **mnt2phenCu8w**) cations per supercell. The Si, Al, and Mg atoms are in yellow, pink, and green colours, respectively. This colour format is extended to the rest of this work. The main non-bonding interactions are shown in dashed lines. (For interpretation of the references to colour in this figure legend, the reader is referred to the Web version of this article.)

periodical box with the phenanthroline-Cu sulfate ion-pair **phenCu2w_sulf** solvated with 8 water molecules (4 for $Cu^{2+}$ cation and 4 for the sulfate anion) for completing the stoichiometry (**phenCu_sulf8w**). Then, we can describe the exchange cation reaction:
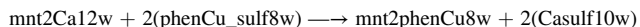
mnt2Ca12w + phenCu_sulf8w ⟶ mntCa6wphenCu4w + Casulf10w
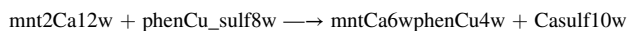
Then, the reaction energy can be calculated as:

$$E = E_{mntCa6wphenCu4w} + E_{Casulf10w} - E_{mnt2Ca12w} - E_{phenCu\_sulf8w}$$

being the exchange cation energy of −97.7 kcal/mol. This value indicates that the phenanthroline-Cu cation is likely to be intercalated in montmorillonite with a favourable energy.

In the same way the reaction of the intercalation of a further phenCu

will be the exchange cation reaction:

mnt2Ca12w + 2(phenCu_sulf8w) ⟶ mnt2phenCu8w + 2(Casulf10w)

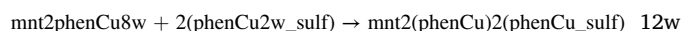Then, the reaction energy can be calculated as:

$$E = E_{\text{mnt2(phenCu)8w}} + 2E_{\text{Casulf10w}} - E_{\text{mnt2Ca12w}} - 2E_{\text{phenCu\_sulf8w}}$$

being the cation exchange energy of −63.1 kcal/mol. This indicates that the formation of the semisaturated hybrid material is likely to be produced according with our experiments. Nevertheless, this energy is lower than that of intercalation of only one complex, possibly due to some steric interactions in the confined interlayer space. This nicely agrees with the experimental fact that the adsorption isotherm is a Frumkin type characterized by a repulsive interaction factor [13], indicative of repulsive interactions among the adsorbed phenCu complex which increase at increasing of the amount of the complex inside the interlayer, meaning that **mntCa6wphenCu4w** is more stable than **mnt2phenCu8w**.

After completing the cation exchange capacity (CEC), our previous experiments indicated that more phenCu complex could be adsorbed in the clay mineral [13]. In this step the adsorption cannot be as a cation exchange but a neutral adsorption of the ion-pair phenCu-sulfate. Then, two phenCu sulfate salts, **phenCu2w_sulf**, were intercalated in montmorillonite, which has already two phenCu$^{2+}$ cations, **mnt2phenCu8w,** described above. Different geometrical dispositions were tested for these complexes in the interlayer and the most stable one was with all phenanthroline rings being parallel to the 001 mineral surface with a d(001) spacing of 17 Å, **mnt2(phenCu)2(phenCu_sulf)12w** (Fig. 3) according

with our experiments (d = 17.1 Å). The more hydrophobic moieties are oriented together forming as a surfactant structure with hydrophobic (phenanthroline rings) and hydrophilic (Cu$^{2+}$ coordination with water molecules and sulfate anions) zones. The phenanthroline rings are in two levels of the interlayer of smectite, but they are not stacking each other, they are displaced (Fig. 3b). One sulfate anion is coordinated with one Cu cation and the other sulfate takes one H atom dissociating from a water molecule, where the resultant OH anion is coordinating one Cu cation (Fig. 3c). One Cu cation interacts electrostatically with one O atom of the mineral surface more negatively charged being close to the tetrahedral Al cation. The water molecules form H bonds with the mineral surface O atoms, with the sulfate O atoms, and with the water O atoms. This complex corresponds to the 'saturated' intercalated compound obtained in our previous experimental work [13]. The Cu$^{2+}$ cation maintains the square-planar coordination being distorted and also is different to that of the phenCu sulfate crystal according with our previous observations with X-ray absorption analysis [13].

This last stage can be represented by the reaction:

mnt2phenCu8w + 2(phenCu2w_sulf) → mnt2(phenCu)2(phenCu_sulf) 12w

Then, the reaction energy can be calculated as:

$$E = E_{\text{mnt2(phenCu)2(phenCu\_sulf)12w}} - E_{\text{mnt2phenCu8w}} - 2E_{\text{phenCu2w\_sulf}}$$

being the exchange cation energy of −78 kcal/mol. Hence, this second intercalation is also energetically favourable. Taking into account the whole of intercalation of all phenanthroline complexes as cation and as sulfate salt forming the saturated hybrid material, the
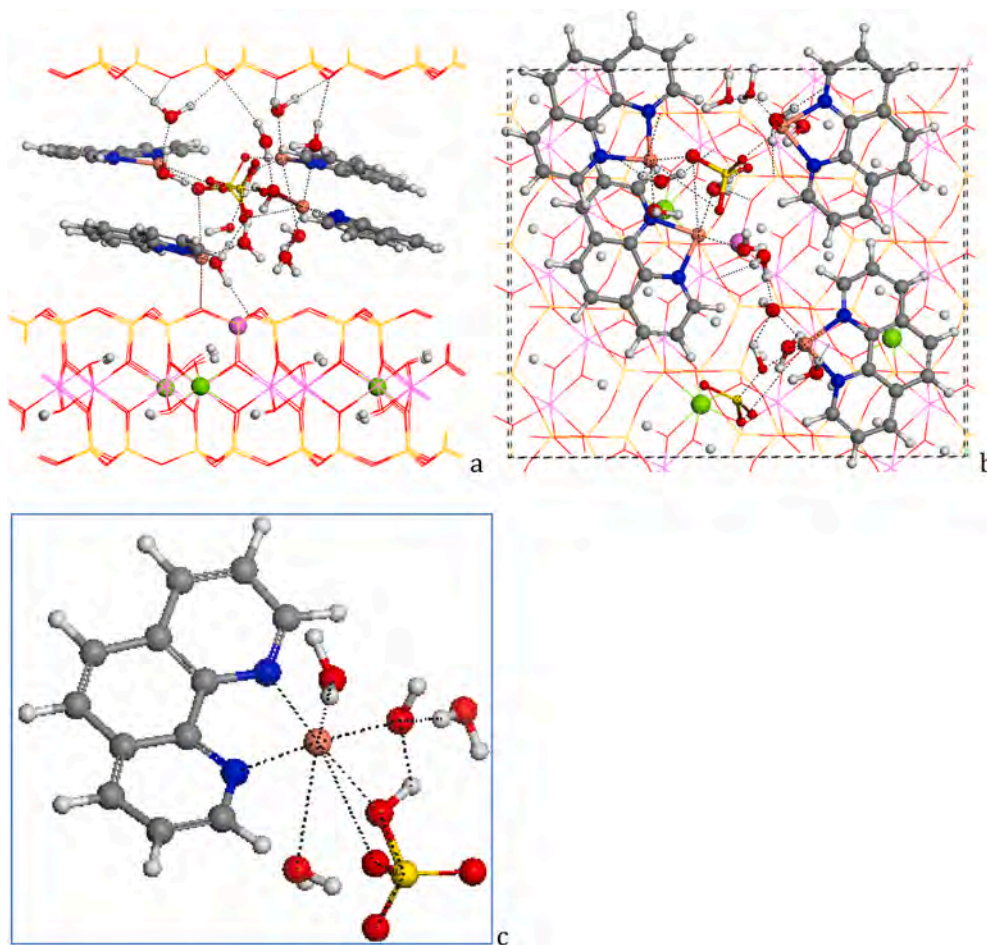


**Fig. 3.** Optimized models of montmorillonite with 2 phenCu$^{2+}$ cations and 2 salts of phenCu sulfate **mnt2(phenCu)2(phenCu_sulf)12w**. View from 010 (a) and 001 (b) planes, and zoom details highlighting the dissociation of one water molecule by one sulfate anion (c). The main non-bonding interactions are shown in dashed lines.

reaction energy is −171.52 kcal/mol. Hence the whole process is also energetically favourable.

### 3.1. Adsorption of ammonia

The adsorption of one molecule of ammonia was calculated in both hybrid materials, the semisaturated and saturated ones (Fig. 4), placing the ammonia molecule randomly in the interlayer space. These optimized structures with ammonia were compared with the initial structure without the adsorption and the ammonia molecule optimized within a periodical box in the same calculation conditions. Then, the adsorption energy was −14.75 and −29.14 kcal/mol in semisaturated and saturated material, respectively, being energetically favourable in both cases. This is consistent with our previous experimental results [13]. In both systems, semisaturated (Fig. 4a), and saturated (Fig. 4c) the ammonia molecule was adsorbed close to the mineral surface forming H bonds between the ammonia H atoms and the surface O atoms. Nevertheless, we prepared an additional model approaching the ammonia molecule close to one Cu cation in the semisaturated system (Fig. 4b). The optimized structure yielded the ammonia molecule coordinating the $Cu^{2+}$ cation, d(HN···Cu) = 2.02 Å, forming at the same time H bonds with the mineral surface, d(NH···OSi) = 2.09–2.30 Å. This complex was 8.5

kcal/mol more stable than the former one. Hence, the adsorption energy of one ammonia molecule for this semisaturated complex can be considered as −23.27 kcal/mol.

In order to explore different adsorption sites of ammonia in the interlayer of smectite, a Monte Carlo simulated annealing method was applied. For that, we explored randomly different positions of the ammonia molecule with different orientations. Using the COMPASS force fields, $10^6$ configurations were explored in each temperature cycle and 10 cycles were performed selecting the 10 most stable final configurations [17]. In all cases the $NH_3$ molecule did not approach to the Cu cation. Probably, repulsive interactions between ammonia and water molecules avoid this approaching. However we found above that the formation of the Cu–$NH_3$ coordination is energetically favourable. Probably the diffusion of the ammonia molecule approaching to the Cu cation is unlikely to observe at the quantum mechanical calculations conditions. Nevertheless, this Cu–$NH_3$ coordination could be formed at room temperature, stabilizing the structure at experimental reaction times, as observed in our previous with nuclear magnetic resonance (NMR) spectroscopy, and X-ray absorption experiments [13].

Following the same method, we generated models adding 2, 3, 4, 5 and 6 ammonia molecules to the semisaturated (**mnt2phenCu8w**) and saturated (**mnt2(phenCu)2(phenCu_sulf)12w**) hybrid materials
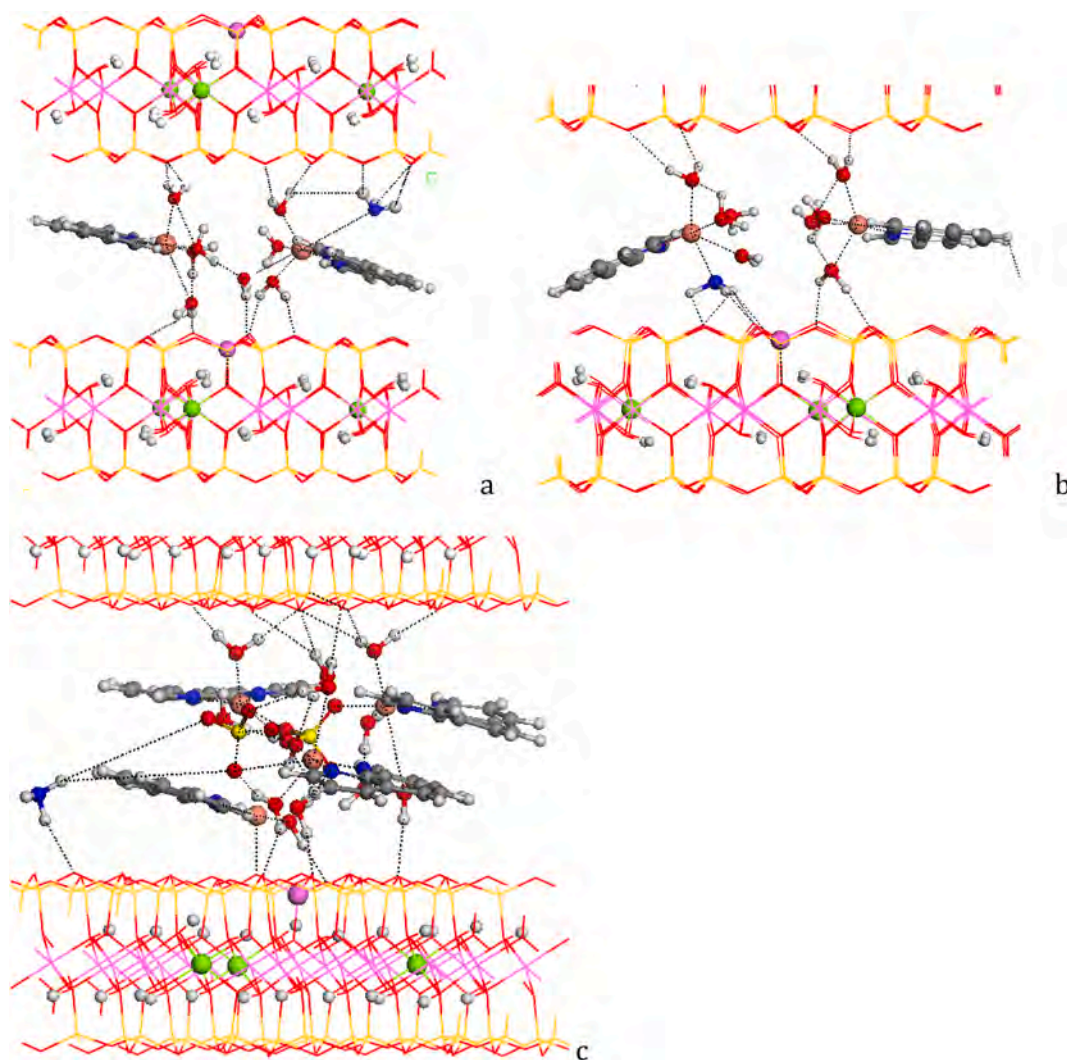


**Fig. 4.** Structured interlayers after adsorption of one ammonia molecule in a montmorillonite 3 × 2 × 1 supercell. (a) Semisaturated material (**mnt2phenCu8w**) with $NH_3$ forming H bonds between H atoms and the surface O atoms. (b) Semisaturated material (**mnt2phenCu8w**) with $NH_3$ coordinated to $Cu^{2+}$. (c) Saturated material (**mnt2(phenCu)2(phenCu_sulf)12w**) with $NH_3$ forming H bonds between H atoms and the surface O atoms. The main non-bonding interactions are shown in dashed lines.

models. In all cases the adsorption energies were negative being energetically favourable (Table 1). This is consistent with our previous experimental results, where the maximum amount of ammonia adsorbed was 1.5 mol $NH_3$ per mol of CuPhen cation in the saturated structure (6 $NH_3$ molecules per 3 × 2 × 1 supercell) and 3 mol $NH_3$ per mol of CuPhen cation in the semi-saturated one (also 6 $NH_3$ molecules per 3 × 2 × 1 supercell).

In the addition of the second ammonia molecule, several options were explored and one of the most stable structure obtained after the optimization is with the ammonia molecules coordinating the $Cu^{2+}$ cations in the semi-saturated hybrid material (Fig. 5a). The coplanar square coordination of $Cu^{2+}$ (with the phenanthroline N atoms and two water molecules) is maintained in both complexes as in the above structures and close to the centre of the interlayer space, with d (CN···Cu) = 1.99–2.03 Å and d($H_2O$···Cu) = 2.23–2.73 Å. However, the entrance of the ammonia molecules produced a distorted coordination sphere in both $Cu^{2+}$ cations, which can be considered as a hepta-coordinated $Cu^{2+}$ cation, with the ammonia adsorbates d(HN···Cu) = 2.23–2.29 Å and the other water molecules d($H_2O$···Cu) = 2.17–2.37 Å. Besides at the same time, these ammonia molecules form H bonds with the mineral surface O atoms d(NH···OSi) = 1.42, 1.76–2.20 Å. Some water molecules form also H bonds with the surface O atoms and d (HOH···OSi) = 1.80–2.38 Å. This structure with the ammonia coordinating the Cu cations can justify its high adsorption energy (Table 1). However, there are many possible adsorption sites of ammonia within the interlayer of clay and many of them are likely to exist thermodynamically at room temperature.

In the saturated hybrid solid model, the ammonia molecules cannot enter to the coordination sphere of $Cu^{2+}$. This can justify its low adsorption energy (−19.10 vs −38.02 kcal/mol) (Table 1). This effect is due to the presence of the sulfate anions that participate in the coordination sphere of the $Cu^{2+}$ cations provoking a certain distortion. One sulfate anion is coordinating to $Cu^{2+}$ with two O atoms forming a hepta-coordinated $Cu^{2+}$ cation along with the two phenanthroline N atoms and 3 water molecules. The other sulfate anion acts as a bridge coordinating with 3 $Cu^{2+}$ cations (see detailed view in Fig. 5b). One ammonia molecule is forming a strong H bond with one water molecule d ($H_3N$···HOH) = 1.56 Å, that is solvating the sulfate anion. At the same time this ammonia molecule is forming H bonds with the mineral surface, d(HNH···OSi) = 2.13–2.35 Å. As above, some water molecules form H bonds with the surface O atoms, d(HOH···OSi) = 1.56, 1.71–1.80, 1.96 Å. The other ammonia molecule does not approach to the $Cu^{2+}$ cation, forming H bonds with the mineral surface.

In the adsorption of 3 ammonia molecules per 3 × 2 × 1 supercell in the semi-saturated **mnt2phenCu8w**, one ammonia is coordinating a $Cu^{2+}$ cation, d(HN···Cu) = 2.17 Å, and forms H bonds with the mineral surface, d(HNH···OSi) = 1.98–2.35 Å. This interaction provokes a distortion in the coordination sphere of $Cu^{2+}$ breaking the coplanar-square form. The other ammonia molecule forms a H bond with a co-ordination water d(HN···HOH) = 1.61 Å and another H bond with the clay surface O atom close to the tetrahedral aluminium, d(HNH···OSi) = 2.11 Å. The third ammonia molecule remains out of the Cu coordination
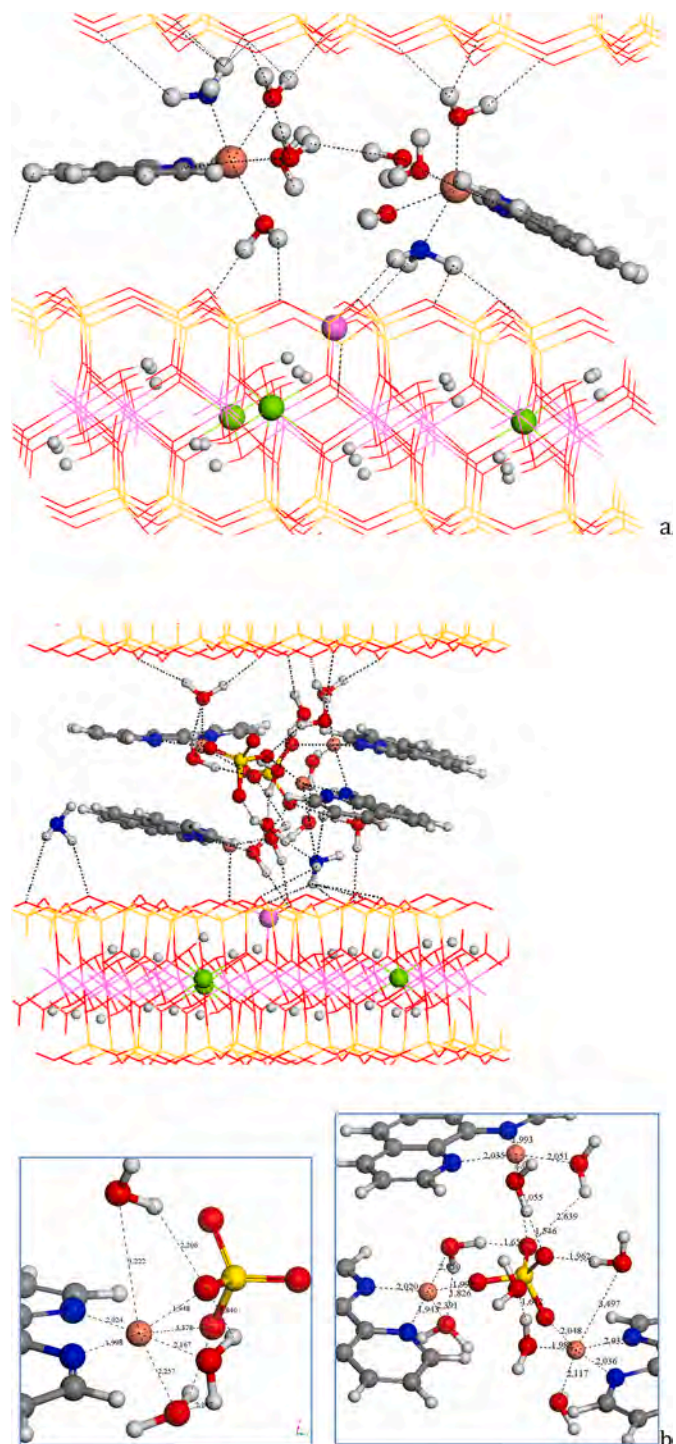


Fig. 5. Structured interlayers after adsorption of two ammonia molecules in the montmorillonite 3 × 2 × 1 supercell. (a) Semisaturated (**mnt2phenCu8w**); (b) Saturated (**mnt2(phenCu)2(phenCu_sulf)12w**) (with two zoom for details of the coordination of sulfate anions) hybrid materials models. The main non-bonding interactions are shown in dashed lines. Distance values are in Å.

zones forming H bonds with the clay surface O atoms d(HNH···OSi) = 2.30–2.77 Å. Some water molecules form also H bonds with the surface O atoms and d(HOH···OSi) = 1.66–1.89 Å (Fig. 6a).

In the saturated solid **mnt2(phenCu)2(phenCu_sulf)12w**, one ammonia molecule interacts with one sulfate anion d(HNH···OSO) = 1.62 Å with a so much strength that withdraws a H atom of a vicinal water molecule forming an ammonium ($NH_4^+$) cation maintaining close

**Table 1**
Adsorption energy of the ammonia molecules in the interlayer space of the semi-saturated and saturated hybrid materials.

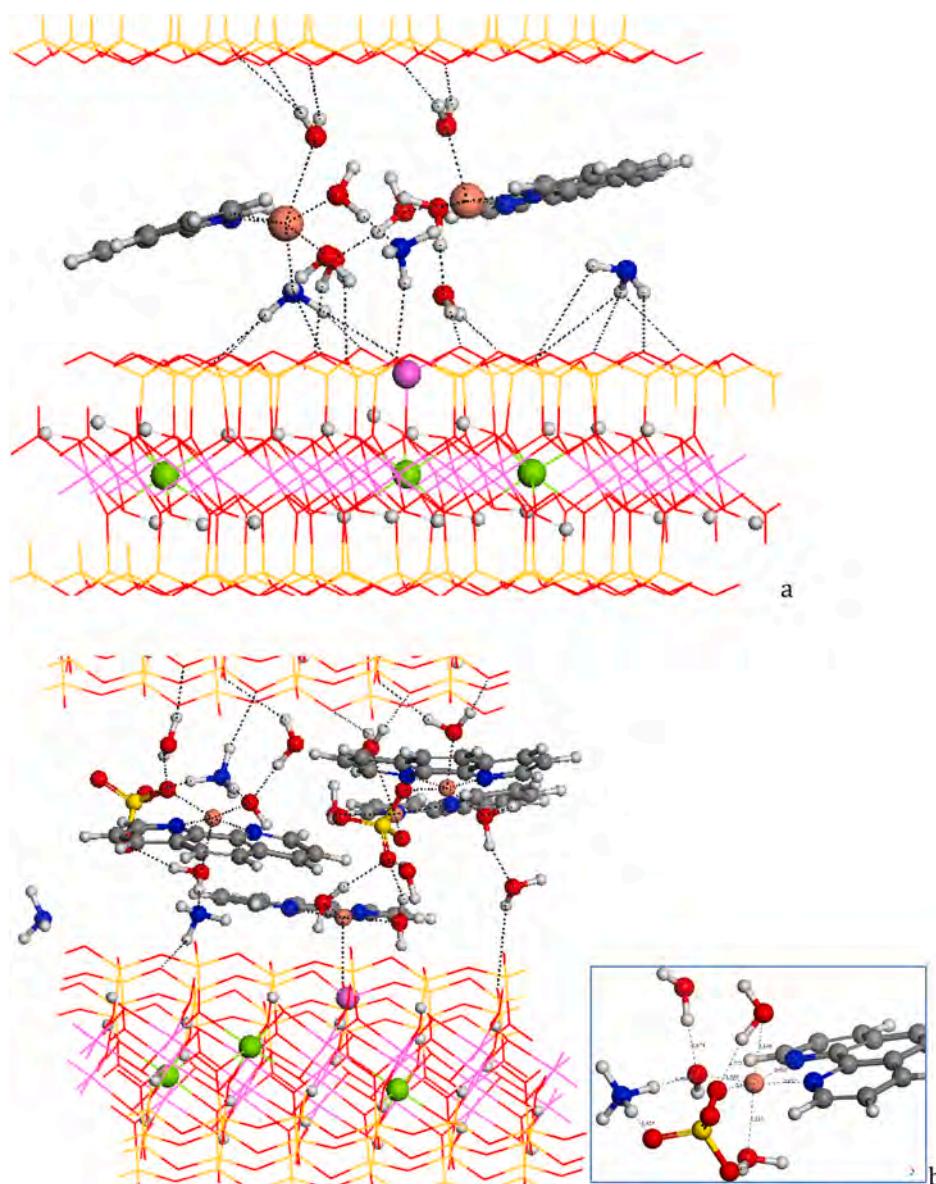| N° $NH_3$ | Adsorption energy (kcal/mol) | |
|---|---|---|
| | mnt2phenCu8w | mnt2(phenCu)2(phenCu_sulf)12w |
| 1 | −14.75 ($H_2N$–H..O–Si)/-23.27 ($H_3N$···Cu) | −29.14 |
| 2 | −38.02 | −19.10 |
| 3 | −29.09 | −45.99 |
| 4 | −18.0 | −19.97 |
| 5 | −28.09 | −29.58 |
| 6 | −29.7 | −17.36 |

**Fig. 6.** Structured interlayers after adsorption of three ammonia molecules in montmorillonite $3 \times 2 \times 1$ supercell. (a) Semisaturated (**mnt2phenCu8w**); (b) Saturated (**mnt2(phenCu)2(phenCu_sulf)12w**) (with a zoom view for details of the formation of ammonium cation) hybrid materials models. The main non-bonding interactions are shown in dashed lines.

to the hydroxy anion, like a ammonium hydroxyl ion-pair, d(HNH···OH) = 1.52 Å (see zoom view in Fig. 6b). This effect can justify the strong adsorption energy in this system (Table 1). Besides, this ammonium cation is stabilized with an additional H bond with the clay surface O atoms d(HNH···OSi) = 2.16 Å. The sulfate anion associated with the ammonium cation is coordinated with one $Cu^{2+}$ cation d(OSO···Cu) = 2.14 Å and interacts with two water molecules by hydrogen bonds d(HOH···OSO) = 1.77–1.83 Å. The other sulfate anion is coordinating two $Cu^{2+}$ cations d(OSO···Cu) = 1.97–2.05 Å and 4 water molecules d(HOH···OSO) = 1.64–1.77 Å. The other ammonia molecules is interacting with one coordination water molecule d(HN···HOH) = 1.60 Å and the clay surface O atoms d(HNH···OSi) = 2.03 Å. The third ammonia molecule is out of the Cu coordination spheres interacting with the mineral surface d(HNH···OSi) = 2.40 Å.

In the case of adsorption of 4 ammonia molecules per $3 \times 2 \times 1$ supercell of the semisaturated hybrid material model, one ammonia per phenCu complex, two ammonia molecules are coordinated to $Cu^{2+}$ cations d(HN···Cu) = 2.03–2.23 Å interacting also with the mineral surface d(HNH···OSi) = 2.13–2.43 Å. The other ammonia molecules are

interacting with the mineral surface O atoms, one of them is forming a strong H bond with one water molecule, d(H₃N···HOH) = 1.612 Å (Fig. 7a). In the optimized structure of the saturated hybrid material model, one ammonium cation is formed like in above sample (Fig. 6b) and no other ammonia molecule is coordinated with any $Cu^{2+}$ cation, and in addition several $Cu^{2+}$ cations are rather close d(Cu···Cu) = 4.36 Å (Fig. 7b). However, these unfavourable facts are compensated with the energetically favourable formation of ammonium cation. This justifies the favourable adsorption energy although is lower than above adsorptions (Table 1).

When the proportion of ammonia adsorption is 5 ammonia molecules per 3x2x1supercell of the semi-saturated hybrid material (**mnt2phenCu8w**), one ammonia molecule becomes an ammonium $NH_4^+$ cation taking a H atom from a water molecule, d(H₃NH···OHCu) = 1.47 Å, which coordinates the $Cu^{2+}$ cation (Fig. 8). Two ammonia molecules coordinate two $Cu^{2+}$ cations, d(H₃N···Cu) = 2.02–2.13 Å. In the saturated hybrid material (**mnt2(phenCu)2(phenCu_sulf)12w**), the ammonium $NH_4^+$ cation is also formed taking one H atom from the water molecule that coordinates the $Cu^{2+}$ cation d(H₃NH···OHCu) =

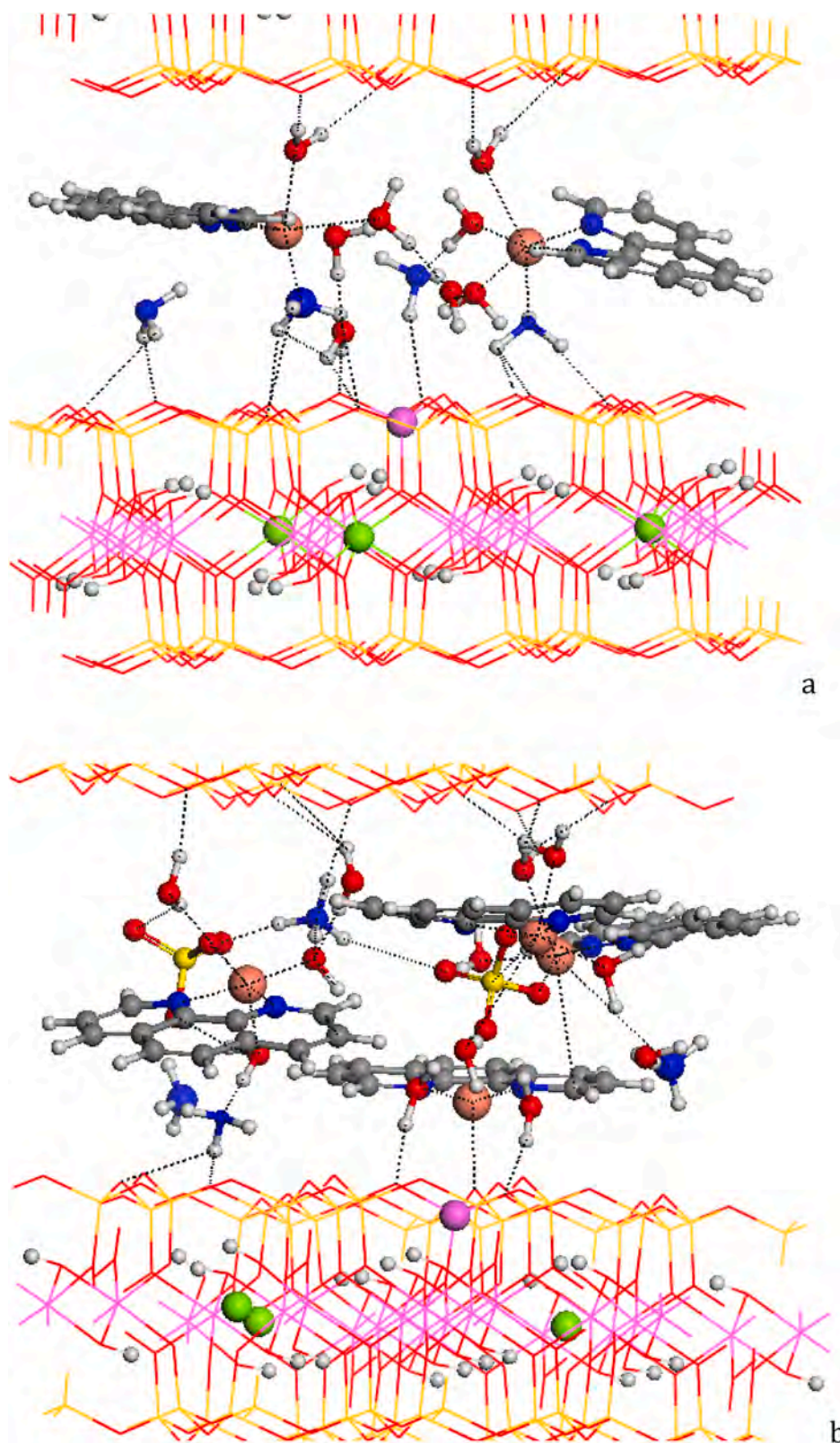**Fig. 7.** Structured interlayers after adsorption of four ammonia molecules permontmorillonite 3 × 2 × 1 supercell. (a) Semisaturated (**mnt2phenCu8w**); (b) Saturated (**mnt2(phenCu)2(phenCu_sulf)12w**) hybrid materials models. The main non-bonding interactions are shown in dashed lines.

1.50 Å (Fig. 8). This ammonium cation forms a strong H bond with one sulfate O atom, d(H₃NH…OS) = 1.66 Å. Other ammonia molecule acts as a bridging molecule between the Cu complex, water molecules, sulfate anion, and clay surface. Besides, two ammonia molecules are

interacting with water molecules with H₃N···H–OH and H₂NH···OH₂ hydrogen bonds.

In the case of an ammonia sorption close to the proportion of 3 times the intercalated phenCu complexes, 6 ammonia molecules per 3 × 2 × 1
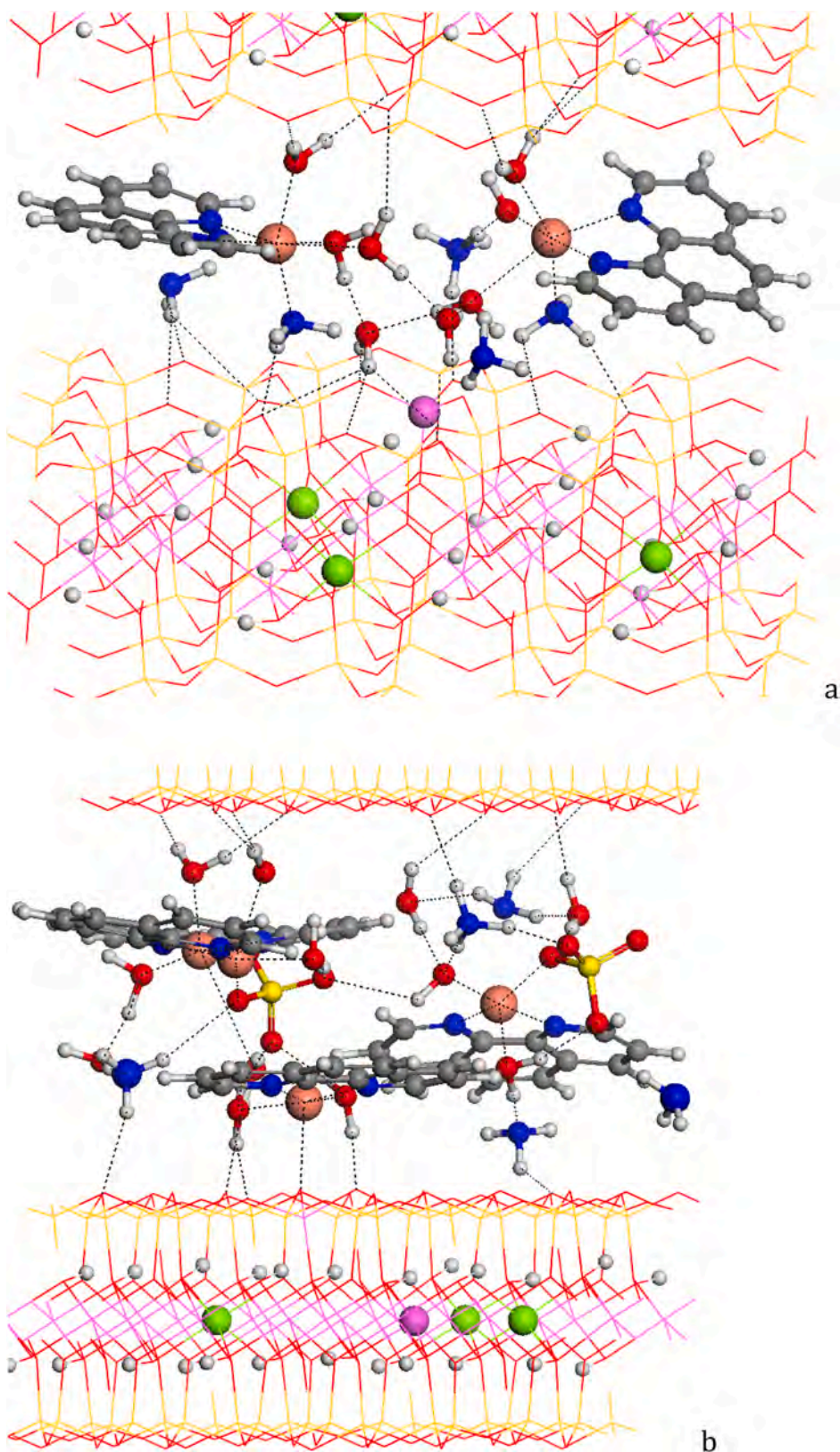
**Fig. 8.** Structured interlayers of the montmorillonite 3 × 2 × 1 supercell after adsorption of five ammonia molecules. (a) Semisaturated (**mnt2phenCu8w);** (b) Saturated (**mnt2(phenCu)2(phenCu_sulf)12w)** hybrid materials models. The main non-bonding interactions are shown in dashed lines.

supercell, three ammonia are coordinating the $Cu^{2+}$ cations in the semisaturated hybrid (**mnt2phenCu8w**) with $d(H_3N \cdots Cu) = 1.99$–$2.00$ Å (Fig. 9a). One $Cu^{2+}$ cation is coordinated by two ammonia molecules forming the opposite vertices of the octahedral coordination sphere. One ammonia is bridging by H bonds between the coordination water d $(H_3N \cdots HOH) = 1.55$ Å and the mineral surface $d(HNH \cdots OSi) = 2.26$–$2.82$ Å. The other ammonia molecules are out of the Cu coordination spheres. As in the above structures, all water molecules are connected by H bonds and some of them are connected with the mineral surface. In the saturated structure, (**mnt2(phenCu)2(phenCu_sulf) 12w**), the $NH_3$/phenCu ratio of 1.5 is satisfied (6 ammonia molecules per 4 phenCu complexes in a $3 \times 2 \times 1$ supercell). One ammonium $(NH_4^+)$ cation is formed $d(H_3N–H) = 1.11$ Å and $d(H_3NH \cdots OH) = 1.51$ Å, taking a proton from one water molecule that is coordinating a $Cu^{2+}$ cation $d(Cu \cdots OH) = 1.94$ Å (Fig. 9b). This ammonium cation is also interacting with one sulfate anion, $d(H_3NH \cdots OSO) = 1.66$ Å and with
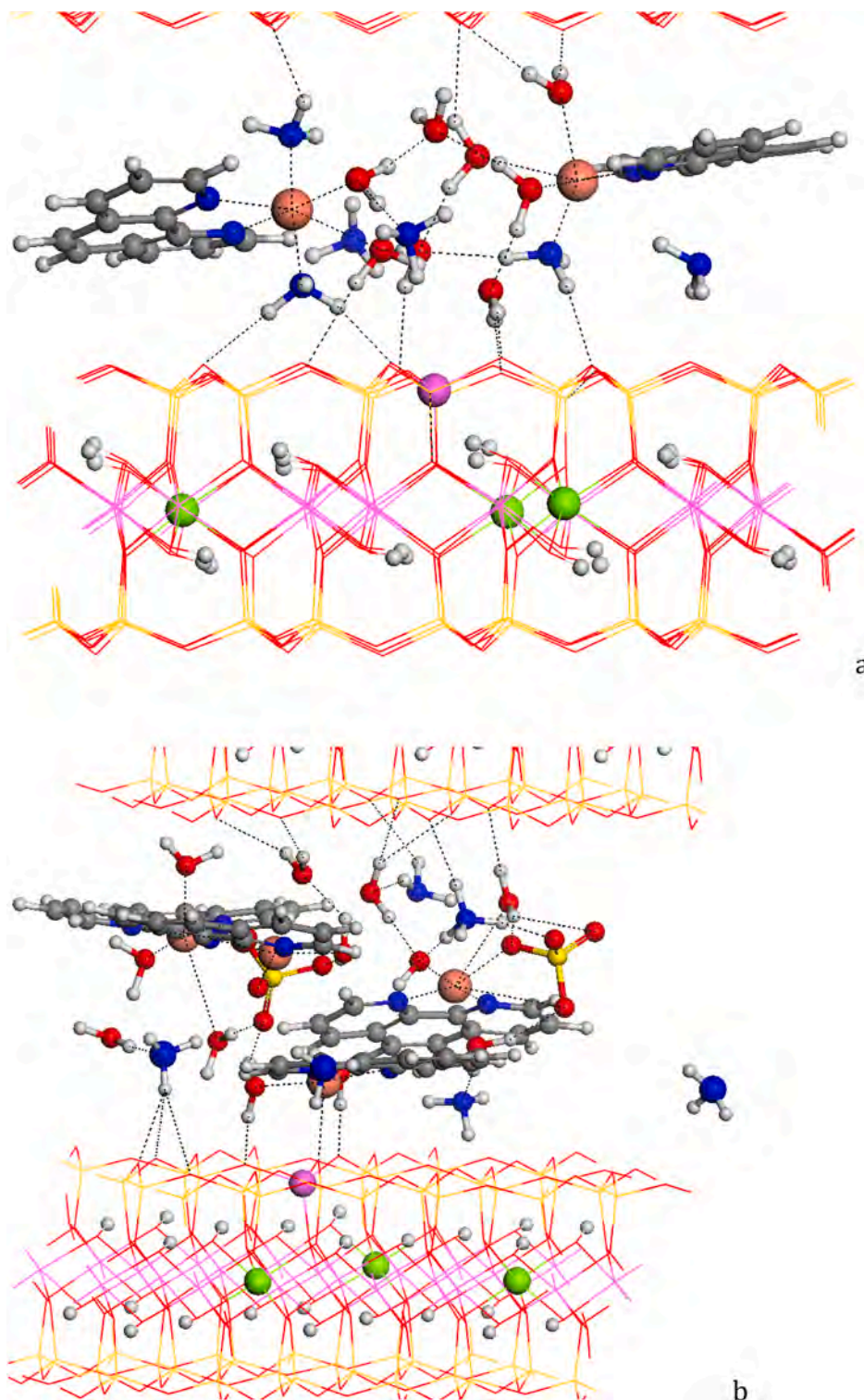


**Fig. 9.** Structured interlayer space after adsorption of six ammonia molecules per montmorillonite $3 \times 2 \times 1$ supercell. (a) Semisaturated (**mnt2phenCu8w**); (b) Saturated (**Mnt2(phenCu)2(phenCu_sulf)12w**) hybrid materials models. The main non-bonding interactions are shown in dashed lines.

the mineral surface, $d(H_3NH\cdots OSi) = 2.04$ Å. In these optimized adsorption models the ammonium cations are formed by exchanging H atoms between ammonia and water molecules according with our previous experimental observations; in particular the broad signal observed in the $^1H$ NMR spectrum of the saturated material at $-4.7$ ppm and attributed to exchanging hydrogens of Cu-coordinated water and ammonia molecules could arise from the strict relationship between ammonia and water in the interlayer as proposed by the calculated model [13]. Three ammonia molecules are interacting with water molecules, $d(H_3N\cdots HOH) = 1.63–2.08$ Å, and mineral surface, $d(H_2NH\cdots OSi) = 2.12–2.30$ Å and the rest two ammonia are out of the Cu coordination spheres interacting with the mineral surface $d(H_2NH\cdots OSi) = 2.61–3.15$ Å. As in the above saturated structure, one sulfate anion is coordinating two $Cu^{2+}$ cations, $d(Cu\cdots OSO) = 1.94–2.07$ Å, and one $Cu^{2+}$ cation is coordinated with minerals surface O atoms, $d(Cu\cdots OSi) = 2.28$ Å. All water molecules are forming a network of H bonds between other water and ammonia molecules and sulfate anions.

## 4. Conclusions

The intercalation of 1,10-phenanthroline-Cu(II) cation in the interlayer space of montmorillonite by cation exchange mechanism is energetically favourable. After reaching the cation exchange capacity of the clay, a further adsorption of phenanthroline-Cu complexes as sulfate salts is also energetically favourable. This is consistent with our previous experimental results. In all cases the phenanthroline rings are more or less parallel to the mineral surface.

The adsorption of ammonia molecules by these hybrid materials is also energetically favourable confirming the experimental results. This ammonia adsorption does not change the spatial disposition of the hydrated phenanthroline-Cu complexes in the interlayer nanospace of smectite, confirming their high stability in montmorillonite. A proton exchange between ammonia and water molecules is possible forming ammonium cations in the nanoconfined interlayer space of montmorillonite, according with our experimental observations. The presence of $Cu^{2+}$ cations facilitates the ammonia adsorption because the coordination of ammonia molecules with the Cu cations is energetically favourable. However, the ammonia molecules interact also with the interlayer surface of the phyllosilicate along with water molecules. Then, these interactions will control the kinetics of the adsorption process. Finally at room temperature, the ammonia molecules can reach the Cu cations by diffusion in the nano-confined space of the hybrid material. This ammonia-Cu coordination increases the stability of the ammonia as ammonium hydroxide species in the hybrid material.

These theoretical results confirm our previous experimental observations validating the theoretical methodology used in this work. These DFT calculations are good tools for helping the interpretation of experimental results and can be extended to other materials and complex systems.

## CRediT authorship contribution statement

**C. Ignacio Sainz-Díaz:** coordination of writing manuscript and DFT calculations. **Elena Castellini:** conceived the original project idea. **Elizabeth Escamilla-Roa:** DFT calculations were performed, All co-authors have approved the final version of the manuscript and have contributed to the edition of the manuscript. **Fabrizio Bernini:** contributed to the experimental work. **Daniele Malferrari:** contributed to the experimental work. **Maria Franca Brigatti:** conceived the original project idea. **Marco Borsari:** conceived the original project idea.

## Declaration of competing interest

The authors declare that they have no known competing financial interests or personal relationships that could have appeared to influence

the work reported in this paper.

## References

[1] S.S.S. Cardoso, J.H.E. Cartwright, J. Čejková, L. Cronin, A. De Wit, S. Giannerini, D. Horváth, A. Rodrigues, M.J. Russell, C.I. Sainz-Díaz, Á. Tóth, Chemobrionics: from self-assembled material architectures to the origin of life, Artif. Life 26 (2020) 315–326.

[2] M.J. Russell, The alkaline solution to the emergence of life: energy, entropy and early evolution, Acta Biotheor. 55 (2007) 133–179.

[3] M.F. Brigatti, D. Malferrari, A. Laurora, C. Elmi, Structure and mineralogy of layer silicates: recent perspectives and new trends, in: M.F. Brigatti, A. Mottana (Eds.), Layered Mineral Structures and Their Application in Advanced Technologies, EMU, Notes in Mineralogy, European Mineralogical Union and the Mineralogical Society of Great Britain, London, 2011, pp. 1–71.

[4] X. Hu, J. Guo, C. Liu, H. Zen, Y. Wang, W. Du, Two new supermolecular structures of organic–inorganic hybrid compounds: $[Zn(phen)(SO_4)(H_2O)_2]_n$ and $[Cu(phen)(H_2O)_2].SO_4$ (phen = 1,10-phenanthroline), Inorg. Chim. Acta. 362 (2009) 3421–3426.

[5] A.A. Schilt, Applications of 1,10-Phenanthroline and Related Compounds, Pergamon Press, Oxford, U.K., 1969.

[6] M.F. Brigatti, C.I. Sainz-Díaz, M. Borsari, F. Bernini, E. Castellini, D. Malferrari, Crystal chemical characterization and computational modeling of a μ-oxo Fe(III) complex with 1,10-phenanthroline clarify its interaction and reactivity with montmorillonite, Rend. Fis. Acc. Lincei 28 (2017) 605–614.

[7] F. Bernini, E. Castellini, D. Malferrari, M. Borsari, M.F. Brigatti, Stepwise structuring of the adsorbed layer modulates the physicochemical properties of hybrid materials from phyllosilicates interacting with the μ-oxo-Fe+3-phenanthroline complex, Microporous Mesoporous Mater. 211 (2015) 19–29.

[8] C.I. Sainz-Díaz, F. Bernini, E. Castellini, D. Malferrari, M. Borsari, A. Mucci, M. F. Brigatti, Experimental and theoretical investigation of intercalation and molecular structure of organo-iron complexes in montmorillonite, J. Phys. Chem. C 122 (2018) 25422–25432.

[9] F. Bernini, E. Castellini, D. Malferrari, G.R. Castro, C.I. Sainz-Díaz, M.F. Brigatti, M. Borsari, Effective and selective trapping of volatile organic sulfur derivatives by montmorillonite intercalated with a μ-oxo Fe(III)−Phenanthroline complex, ACS Appl. Mater. Interfaces 9 (2017) 1045–1056.

[10] D. Malferrari, E. Castellini, F. Bernini, A. Serrano-Rubio, G.R. Castro, C.I. Sainz-Díaz, M. Caleffi, M.F. Brigatti, M. Borsari, Chemical trapping of gaseous $H_2S$ at high and low partial pressures by an iron complex immobilized inside the montmorillonite interlayer, Microporous Mesoporous Mater. 265 (2018) 8–17.

[11] E. Castellini, D. Malferrari, F. Bernini, C.I. Sainz-Díaz, A. Mucci, M. Sola, M. F. Brigatti, M. Borsari, Trapping at the solid-gas interface: selective adsorption of naphthalene by montmorillonite intercalated with a Fe(III)-phenanthroline complex, ACS Omega 4 (2019) 7785–7794.

[12] E. Castellini, F. Bernini, L. Sebastianelli, C.I. Sainz-Díaz, A. Serrano, G.R. Castro, D. Malferrari, M.F. Brigatti, M. Borsari, Interlayer-confined Cu(II) complex as an efficient and long-lasting catalyst for oxidation of $H_2S$ on montmorillonite, Minerals 10 (2020) 510.

[13] E. Castellini, D. Malferrari, F. Bernini, B. Bighi, A. Mucci, C.I. Sainz-Díaz, A. Serrano, G.R. Castro, M.F. Brigatti, M. Borsari, A new material based on montmorillonite and Cu (II)-phenanthroline complex for effective capture of ammonia from gas phase, Appl. Clay Sci. 184 (2020) 105386.

[14] S.J. Clark, M.D. Segall, C.J. Pickard, P.J. Hasnip, M.J. Probert, K. Refson, M. C. Payne, First principles methods using CASTEP, Z. Kristallogr. 220 (2005) 567–570.

[15] B. Delley, Hardness conserving semilocal pseudopotentials, Phys. Rev. B Condens. Matter 66 (2002) 155125.

[16] A. Tkatchenko, M. Scheffler, Accurate molecular van der waals interactions from ground-state electron density and free-atom reference data, Phys. Rev. Lett. 102 (2009), 073005.

[17] Materials Studio Biovia, Dassault Systems, 2018.

[18] A. Borrego-Sánchez, C. Viseras, C. Aguzzi, C.I. Sainz-Díaz, Molecular and crystal structure of praziquantel. Spectroscopic properties and crystal polymorphism, Eur. J. Pharmaceut. Sci. 92 (2016) 266–275.

[19] C.I. Sainz-Díaz, A. Villacampa, F. Otálora, Crystallographic properties of the calcium phosphate mineral, brushite, by means of First Principles calculations, Am. Mineral. 89 (2004) 307–313.

[20] E. Escamilla-Roa, M.-P. Zorzano, J. Martin-Torres, A. Hernández-Laguna, C. I. Sainz-Díaz, DFT study of the reduction reaction of calcium perchlorate on olivine

surface: implications to formation of Martian's regolith, Appl. Surf. Sci. 512 (2020) 145634.

[21] J. Ortega-Castro, N. Hernández-Haro, M.T. Dove, A. Hernández-Laguna, C.I. Sainz-Díaz, Density functional theory and Monte Carlo study of octahedral cation ordering of Al/Fe/Mg cations in dioctahedral 2:1 phyllosilicates, Am. Mineral. 95 (2010) 209–220.

[22] E. Castellini, F. Bernini, M. Borsari, M.F. Brigatti, G.R. Castro, D. Malferrari, L. Medici, A. Mucci, Baseline studies of the clay minerals society source clay montmorillonite STx-1b, Clay Clay Miner. 65 (2017) 220–233.

[23] J. Ortega-Castro, N. Hernández-Haro, A. Hernández-Laguna, C.I. Sainz-Díaz, DFT calculation of crystallographic properties of dioctahedral 2:1 phyllosilicates, Clay Miner. 43 (2008) 351–361.

[24] V. Timón, C.I. Sainz-Díaz, V. Botella, A. Hernández-Laguna, Isomorphous cation substitution in dioctahedral phyllosilicates by means of ab initio quantum mechanical calculations on clusters, Am. Mineral. 88 (2003) 1788–1795.